

# Studies on the Unsteady Boundary Layer on a Flat Plate Subjected to Incident Wakes\* (Forced Transition Models of the Boundary Layer)

Ken-ichi FUNAZAKI\*\*, Toshikatsu MEGURO\*\*\*  
and Shigemichi YAMAWAKI\*\*\*\*

Detailed studies are conducted to investigate the effects of the incident wakes generated by rotating circular cylinders on the characteristics of the transitional boundary layer developing on a flat plate. In this report, the primary concern is to measure the time-averaged heat transfer distribution along the flat plate under several conditions of wake characteristics and cylinder speeds. The obtained data are then utilized in the development of a simple but accurate model for an intermittency factor of the transitional boundary layer subjected to the incoming wakes. Two transition models, the Mayle-Dullenkopf model and a geometrical intermittency factor model, i.e., a modified Pfeil model, are employed for comparison with the measured heat transfer data, and it is found that the latter model, which only considers evolution of the turbulent spot in the space-time domain, yields a better prediction.

**Key Words:** Unsteady Flow, Boundary Layer, Wake, Heat Transfer Measurement, Transition Model, Turbomachinery

## 1. Introduction

Effects of wake/blade interaction phenomena in turbomachines have been studied mostly from the viewpoint of blade vibration or noise generation. Recently, they have attracted a great amount of attention from various researchers because it has become known that wake/blade interaction affects the stage efficiency and increases heat load on the blade much more than was expected from steady flow analysis; hence a number of relevant studies have been carried out up to date<sup>(1)-(6)</sup>.

It is easily understood that transition of the boundary layer on the blade surface plays an important role in wake/blade interaction. Using Emmons' concept of the transition process of the boundary

layer<sup>(6)</sup> and the subsequent work of Narasimha<sup>(7)</sup>, Mayle and Dullenkopf<sup>(8),(9)</sup> proposed a transition model for the boundary layer that is affected by periodic wakes. Their transition model seems to work very well, but the validity of their data and of the process that they employed in deriving the expression of their model is rather uncertain. Furthermore, they neglected to show the means by which the starting point of the forced transition should be specified when applying their model.

Our study is aimed at verifying the validity of the Mayle-Dullenkopf model and at construction of a forced transition model through detailed measurements of not only the time-averaged heat transfer characteristics but also the unsteady behavior of the boundary layer on a flat plate that is subjected to incident wakes. Experimental simulation is achieved using a wake generator located upstream of the plate, which consists of a belt-driven rotating disk and several circular cylinders on the disk rim. Similar experimental studies have been carried out by several researchers, most of whom employ test facilities that consist of stationary linear/annular cascades and moving circular cylinders in front of the cascades.

\* Received 20th August, 1992. Paper No. 91-1584

\*\* Department of Mechanical Engineering, Iwate University, 3-5 Ueda 4-chome, Morioka 020, Japan

\*\*\* Motoyama Engineering Works, Ltd., 12-1 1-chome, Tsutsumi-machi, Aoba-ku, Sendai 981, Japan

\*\*\*\* Ishikawajima - Harima Heavy Industries, Ltd., Tonogaya, Mizuho-machi, Nishitama-gun, Tokyo 190-12, Japan

With these cascade-type facilities, however, the effect of blade surface curvature or external flow acceleration/deceleration is also included in the measured data, which makes the situation more complicated so that it is difficult to understand the wake effect itself. In this study, in contrast with those works, a flat plate is used for the simulation of wake/blade interaction because it is considerably easier to conduct detailed measurement of the boundary layer under controlled flow conditions, for example, free-stream turbulence intensity. Another benefit of using the flat plate is that it is relatively easy to detect the wake effect solely from the obtained results, which is critical to the modeling of the forced transition of the boundary layer.

### Nomenclature

- $C$ : Mayle-Dullenkopf coefficient (=1.9)  
 $k$ : reduced frequency  
 $h$ : heat transfer coefficient  
 $L$ : length of the flat plate  
 $n$ : revolution  
 $n_c$ : number of cylinders  
 $Re_x$ : Reynolds number based on the length measured from the leading edge of the plate  
 $Re_\theta$ : momentum thickness Reynolds number  
 $St$ : Stanton number  
 $Tu$ : ensemble-averaged turbulence intensity  
 $U_E, U_F$ : trailing edge and leading edge propagation velocities of turbulent spot  
 $U_\infty$ : free-stream velocity  
 $\bar{v}(t_j)$ : ensemble-averaged velocity  
 $x_{TW}$ : starting point of forced transition  
 $\gamma(x)$ : intermittency factor  
 $t$ : incoming wake period  
 $\tau_w$ : wake duration

## 2. Theoretical Consideration of the Wake-Induced Boundary Layer Transition

### 2.1 Effect of velocity fluctuation

Because of the possibility of transition induced by the velocity fluctuation ( $\Delta U$ ) associated with incident wakes, the unsteady Reynolds number of the boundary layer, which is defined by

$$Re_{us} = \frac{U_\infty \Delta U}{\nu \omega} = \frac{U_\infty C}{\nu \omega C} \frac{U_\infty \Delta U}{U_\infty} = Re \frac{1}{k} \frac{\Delta U}{U_\infty},$$

is calculated for the simulated flow condition in the present study, where  $Re$  is the Reynolds number for the free-stream and  $k$  is the reduced frequency for the unsteady flow, both of which are based on the main flow characteristics. Rough estimation of the unsteady Reynolds number, under the assumption that  $Re \approx 10^6$ ,  $k \approx 10$  and  $\Delta U/U_\infty \approx 10^{-1}$ , which are typical values encountered in modern aero-engines, yields  $Re_{us} \approx 10^4$ . According to the experiments by Obremski and

Fejer<sup>(4)</sup>, in the case of unsteady Reynolds numbers lower than  $2.5 \times 10^4$ , transition cannot be caused by the velocity fluctuation. Therefore, in the following the effect of the velocity fluctuation on the transition phenomena is ignored.

### 2.2 Intermittency factor of the unsteady boundary layer

According to the conventional approach for investigation of natural transition phenomena, an intermittency factor defined for the wake-forced transitional boundary layer,  $\gamma(x)$ , is introduced in this study.

**2.2.1 Pfeil model** Pfeil et al.<sup>(1)</sup> previously proposed a forced transition model in terms of the intermittency factor. In this model, incoming wakes with period  $\tau$  stimulate the boundary layer due to their high turbulence intensity, creating new high-turbulence areas in the boundary layer, so-called "forced" turbulent spots, beneath the wakes. These turbulent spots then move downstream in the same manner as a natural turbulent spot, and are elongated in the streamwise direction due to the difference between the propagation speeds of the leading and the trailing edges of the spots<sup>(10)</sup>, which are referred to as  $U_F = (\beta_F U_\infty)$  and  $U_E = (\beta_E U_\infty)$ , respectively. This situation is schematically represented in Fig. 1, in which the turbulent regions associated with the turbulent spots evolves in the time-space domain. In this case, the intermittency factor at an arbitrary position  $x$  can be defined by the length of time during which the turbulent region exists. The ensemble-averaged intermittency factor  $\gamma(x)$ , depicted in Fig. 1, is accordingly given by

$$\gamma(x) = \left( \frac{1}{U_E} - \frac{1}{U_F} \right) \frac{x - x_{TW}}{\tau} = \left( \frac{1}{\beta_E} - \frac{1}{\beta_F} \right) \frac{x - x_{TW}}{U_\infty \tau}, \quad (1)$$

where  $x_{TW}$  denotes the point at which the turbulent spot occurs. Note that  $\gamma(x)$  is set to be unity after the two successive turbulent spots merge, which indicates the end of the forced transition process of the boundary layer.

**2.2.2 Mayle-Dullenkopf model** Mayle and Dullenkopf<sup>(8),(9)</sup> proposed a forced transition model,

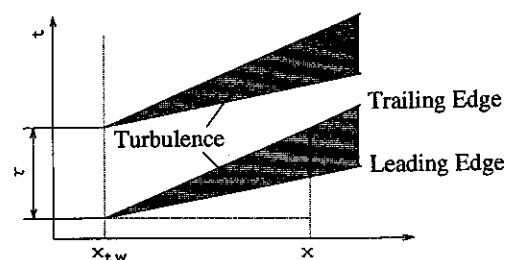


Fig. 1 Schematic representation of the evolution of turbulent spots in the time-space domain

taking into account the contribution from the natural transition based on the well-known works done by Narasimha. Their model is given as follows:

$$\gamma(x) = 1 - \exp \left[ -0.412 \left( \frac{x - x_{TN}}{x_{75} - x_{25}} \right) \right] \times \exp \left[ -b \left( \frac{\tau_w}{\tau} \right) \left( \frac{x - x_{TW}}{U_s} \right) \right], \quad (2)$$

where  $x_{25}$  and  $x_{75}$  are the streamwise positions of  $\gamma = 0.25$  and  $\gamma = 0.75$  measured from the starting point of the natural transition process ( $x_{TN}$ ), respectively,  $b$  represents the value proportional to the generation rate of turbulent spots and  $U_s$  is the average propagation speed of the spots. In the case of low free-stream turbulence intensity, the contribution from the natural transition in Eq. (2) can be ignored, so that the intermittency factor for the forced transition process may be modified as

$$\gamma(x) = 1 - \exp \left[ -b \left( \frac{\tau_w}{\tau} \right) \left( \frac{x - x_{TW}}{U_s} \right) \right], \quad (3)$$

In Eq. (3), which is seemingly simple, there are two unknowns to be determined: the coefficient  $b$  and the initial point of the forced transition process  $x_{TW}$ . Mayle and Dullenkopf showed the following relationship involving the coefficient  $b$ :

$$(b/U_s)(\tau_w U) \cong 1.9,$$

which was reportedly derived from dimensional analysis using relevant experimental data appearing in the literature. Therefore Eq. (3) can be written as

$$\gamma(x) = 1 - \exp \left[ -C \left( \frac{x - x_{TW}}{U_s \tau} \right) \right], \quad C = 1.9. \quad (4)$$

Although Mayle and Dullenkopf insisted that Eq. (4) could yield excellent agreement with the experimental data used, the present authors are somewhat doubtful of the applicability of Eq. (4) to any other case. This is because, firstly, Mayle and Dullenkopf utilized a limited amount of data in deriving Eq. (4), and secondly, values of the data cited in their paper, e.g., the wake duration  $\tau_w$ , were not directly indicated in the original papers, and are indeed difficult to measure.

### 3. Experimental investigation

#### 3.1 Test apparatus

Figure 2 shows the test apparatus used in this study. Air from the nozzle with turbulence intensity of about 0.5% is fed to the test section through the wake generator, as shown in Fig. 3. This wake generator

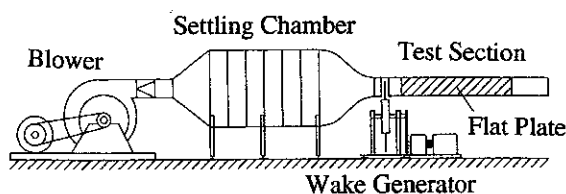


Fig. 2 Test apparatus

consists of a rotating disk with diameter of 400 mm and up to 6 circular cylinders which can be attached on the disk's rim. The test section is a rectangular acrylic duct with 120 mm  $\times$  240 mm cross section and has slots through which the cylinders can pass. Rotating speed of the disk is changeable with a transmission gear box connected to the induction motor, and is sensed by an optical tachometer. Flow rate through the test section can be controlled by the valve of the blower intake and is monitored by a Pitot tube installed at the duct.

A sharp-edged flat plate of 1000 mm length and 10 mm thickness is employed for the measurement of the heat transfer rate; it is placed within the duct aligned almost along its center line. Sixty equally spaced holes of 5 mm diameter are drilled through the plate along the center line. Each of the holes is plugged with urethane foam and a hot junction of a K-type (chromel - alumel) thermocouple is then flush-mounted on the surface to be measured, penetrating back through the foam as shown in Fig. 4. The wires of the thermocouples are buried inside a slot on the back of the plate. Both sides of the plate are covered with stainless steel foil adhesive tapes of 20  $\mu$ m thickness, which are soldered onto copper plates and heated by electricity. For the purpose of preventing the buckling of the foils during heating, transparent tapes (3M Book Tape 845, 90  $\mu$ m thickness) is pasted on the stainless foils. Estimated heat drop through the tape is about 0.025°C.

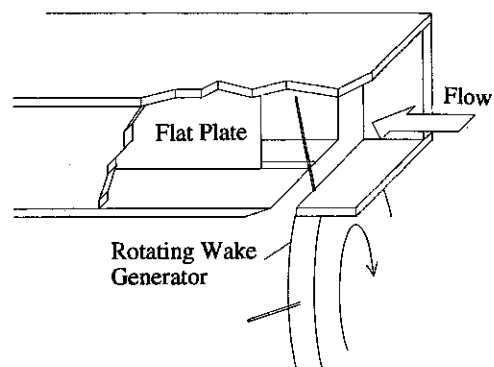


Fig. 3 Wake generator and test section

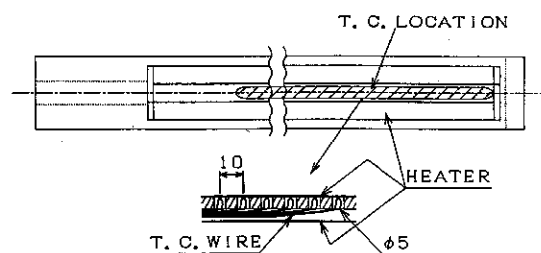


Fig. 4 Flat plate implemented with thermocouples and stainless foils

The distance between the plate and the wake generator can be changed to vary wake characteristics, e.g., wake depth, on the flat plate. Smooth inflow to the flat plate is achieved by adjusting the open area of the duct exit, which is confirmed by the oil flow pattern on the plate.

### 3.2 Measuring system

**3.2.1 Wake characteristics** Figure 5 shows the entire measuring system employed in this study. The I-type hot-wire probe (Kanomax, Model 0251 R) is used not only to detect the wake profile in front of the flat plate, but also to investigate the streamwise variation of wake characteristics above the plate, as shown in the upper part of Fig. 5. Signals from the hot-wire probe are processed by a constant-temperature anemometer (Kanomax, System 7201) and the linearized signals are then A/D-converted by a computer-controlled digitizer (Autonix, APC-204), of which sampling frequency is set to be 50-100 kHz and memory size of the logged data per process is 2 048 word. The above process is triggered by a signal from the optical tachometer, which is synchronized with the disk revolution.

For one test condition, 256 lines of time-serial digitized data for velocity,  $v_i(t_j)$  ( $j=1, \dots, 2\,048$ ), are

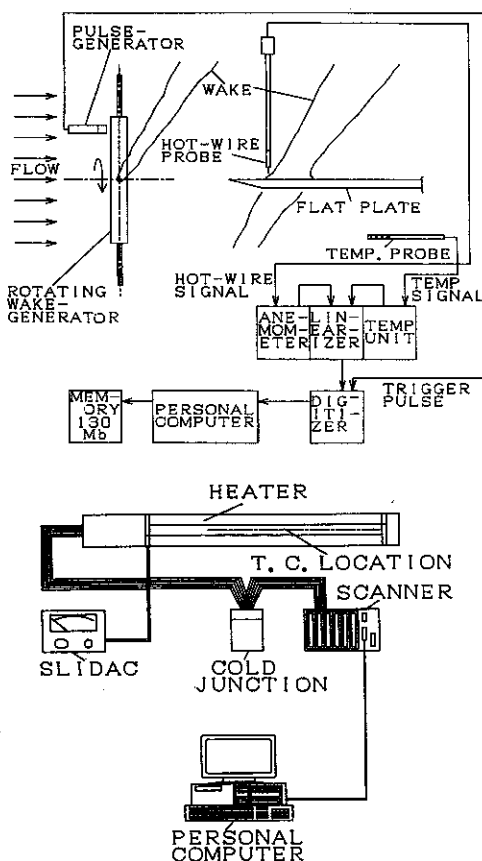


Fig. 5 Measuring system for wake characteristics (upper) and heat transfer characteristics (lower)

logged. They are transferred back to the computer, and then stored in the auxiliary memory unit for subsequent off-line calculation, as described in the following.

Ensemble averaged velocity  $\bar{v}(t_j)$  and its variance  $v'^2(t_j)$  are calculated as

$$\bar{v}(t_j) = \frac{1}{n} \sum_{i=1}^n v_i(t_j), \quad n=256 \quad (5)$$

$$v'^2(t_j) = \frac{1}{n-1} \sum_{i=1}^n [v_i(t_j) - \bar{v}(t_j)]^2 \quad (6)$$

Local turbulence intensity is then defined as

$$Tu(t_j) = \frac{\sqrt{v'^2(t_j)}}{U_\infty} \quad (7)$$

**3.2.2 Heat transfer** After confirming heat balance conditions by monitoring the surface temperature distribution, the signals from the thermocouples embedded in the flat plate are scanned 10 times during about 30 seconds. They are then averaged for each measuring point to obtain time-averaged heat transfer characteristics, i.e., Stanton number distribution  $St$  or heat transfer coefficient distribution  $h$ , which are determined as follows,

$$St = \frac{\dot{q}_w}{C_p U_\infty (T_w - T_\infty)} \quad (8)$$

$$h = \frac{\dot{q}_w}{(T_w - T_\infty)} \quad (9)$$

where  $T_w$  is the averaged surface temperature,  $T_\infty$  is free-stream temperature measured by the temperature-compensation unit located at the aft portion of the test section and  $\dot{q}_w$  is the surface heat flux. Uncertainty in the Stanton number is estimated according to the standard method<sup>(11)</sup> and is around  $\pm 7\%$ .

## 4. Results

### 4.1 Wake characteristics

Before examination of the wake effect on the Stanton number distribution on the plate, it is necessary to understand the unsteady flow field near the plate induced by periodic incoming wakes. Measuring points of the wake are schematically shown in Fig. 6. Figure 7 shows typical profiles of the ensemble-averaged wake velocity and local turbulence intensity measured in front of the flat plate (point A in Fig. 6). Attained peak value of the turbulence intensity within the wake is found to be about 6%, while background turbulence intensity is about 0.65%. Note that the

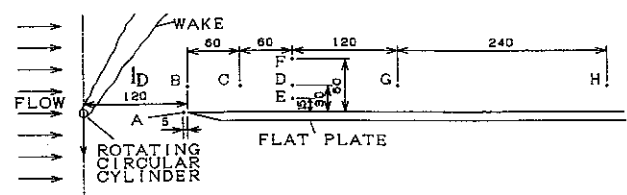


Fig. 6 Positions of wake measurement

Reynolds number based on the diameter of the circular cylinder is  $10^3$ - $10^4$ , so that the drag coefficient can be regarded as constant. Variations of the wake characteristics in the streamwise direction as well as in the direction normal to the flat plate appear in Figs. 8(a) and (b), respectively. It is clear from Fig. 8(a) that both the wake depth and the peak value of the turbulence intensity decay downstream along the flat plate, but they still remain distinguishable even far downstream from the rotating cylinder, e.g., at point  $H(x/d=300)$ . On the other hand, one can notice from Fig. 8(b) that as the hot-wire probe approaches the plate surface, the detected velocity profile varies considerably, while the profile of the turbulence intensity and the wake width in time do not change very much. Some increases in magnitude appear in the velocity profile preceding the velocity defect. This is the case especially for data measured at points closer to the surface. This could be attributed to the wake-plate interaction phenomena pointed out by Meyer<sup>(12)</sup> using the negative jet model. From these observations, it

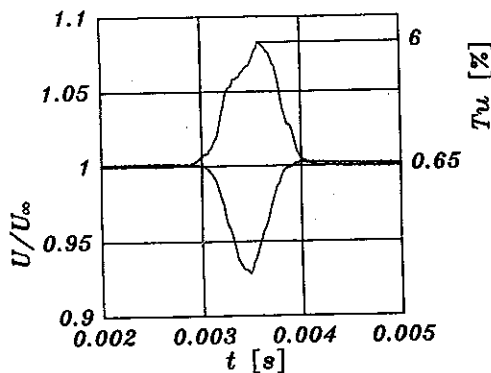
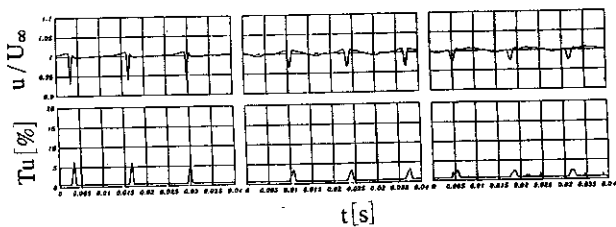
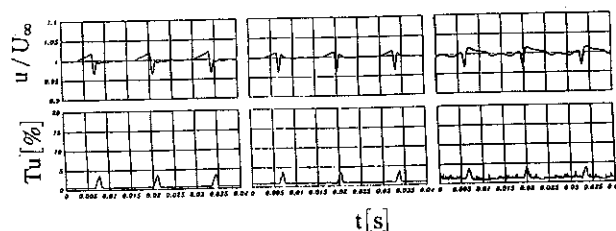


Fig. 7 Typical ensemble-averaged profiles of wake velocity and turbulence intensity within the wake



(a) variation in the flow direction



(b) variation in the crosswise direction

Fig. 8 Variations of the wake profiles ( $n=1500$  rpm,  $n_c=3$ )

can be concluded that the wake width, in other words, wake duration near the surface, cannot be estimated in terms of velocity profile due to its deformation. This indicates that one should define the wake duration, which plays an important role in wake-induced unsteady boundary layer transition, in terms of turbulence intensity involved in the wake, not in terms of velocity.

4.2 Heat transfer

Free-stream velocity was kept at 30 m/s (Reynolds number based on the plate length is  $2 \times 10^6$ ) in this study. Figure 9 shows several curves of Stanton number distributions on the flat plate under the influence of the wakes incoming from the circular cylinders with different wake frequencies, in conjunction with the curves of the fully turbulent condition ( $St_t$ ) and the laminar condition ( $St_l$ ), where the wake incoming frequency  $f$  is defined as

$$f = \frac{nn_c}{60}, \tag{10}$$

where  $n$  is a rotational speed of the disk and  $n_c$  is a cylinder number. Three cylinders are installed on the disk rim ( $n_c=3$ ) and the rotational speed varies from 900 - 1500 rpm. Then, the corresponding range of the reduced frequency  $k$ , that is

$$k = \frac{2\pi f L}{U_\infty}, \tag{11}$$

is 9.4-15.7, which is often encountered in actual engine conditions. The axial distance between the cylinder and the plate is 0.12 m. It should be noted that the fully turbulent boundary condition is established by fixing one of the cylinders in front of the leading edge of the plate so that its wake covers the plate surface continuously. As for the Stanton number distribution of the laminar boundary layer, steady transition starts at  $Re_x \approx 8 \times 10^5$  ( $x/L \approx 0.4$ ) and then ends around  $Re_x \approx 10^6$ .

It is evident from Fig. 9 that the wakes from the rotating cylinders cause earlier transition of the boundary layer so that the curves of the Stanton number exhibit the transitional features of the boundary layer over the measurement region. As the

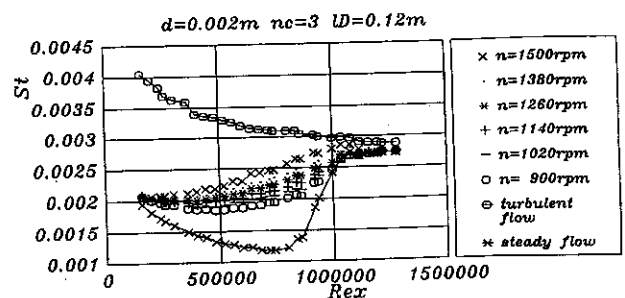


Fig. 9 Time-averaged Stanton number distributions for various wake frequencies

rotational speed increases, the curves tend to shift upward, approaching the curve for the fully turbulent condition. Because the time-averaged Stanton number  $\overline{St}$  can be expressed as

$$\overline{St}(x) = (1 - \gamma(x))St_L(x) + \gamma(x)St_T(x), \quad (12)$$

and the intermittency factor increases as the wake frequency rises, these results are not very surprising. One might notice that the change in the rotational speed also causes some change in the wake characteristics due to increase in relative inlet flow velocity against the cylinder. To verify such an effect on the time-averaged heat transfer, the results of the two test cases are compared in Fig. 10, where combinations of  $n$  and  $n_c$  are different but the wake frequency is the same. Consequently, it is found that the two curves of the measured time-averaged heat transfer coincide. Therefore, one can conclude that one of the dominant factors in the unsteady heat transfer is the wake frequency. This is also supported by close investigation of the wake duration  $\tau_w$ , which indicates that the wake duration measured in front of the leading edge of the plate differs little over the range of rotational speeds of the cylinder in this case.

As for the higher wake frequency cases with 6 cylinders, as seen in Fig. 11, the length of the forced transition process becomes considerably short and the transition ends rapidly around  $Re_x \cong 6 \times 10^5$ . After the end of the transition, the level of the time-averaged

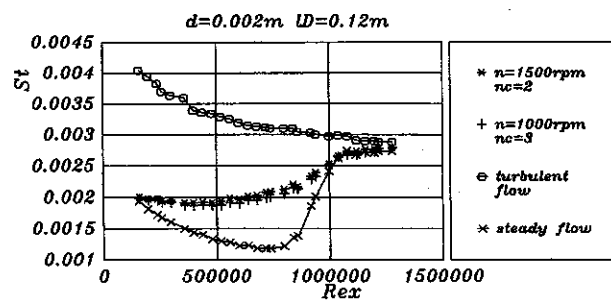


Fig. 10 Time-averaged Stanton number distributions for the cases of ( $n=1500$  rpm,  $n_c=2$ ) and ( $n=1000$  rpm,  $n_c=3$ ), both of which generate unsteady flow of the same wake frequency

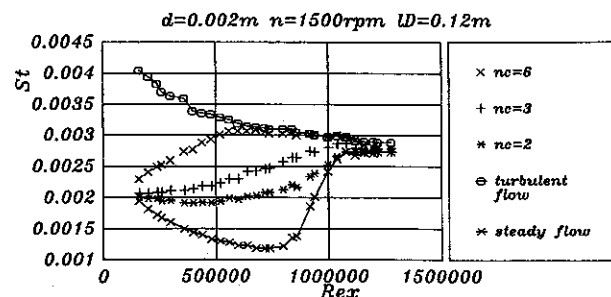


Fig. 11 Time-averaged Stanton number distributions for higher wake frequencies

heat transfer of the unsteady boundary layer almost coincides with that of the fully turbulent boundary layer.

Further investigation is conducted by changing the distance between the cylinder and the leading edge of the plate ( $l_b$ ) in order to examine the effect of the wake characteristics, e.g., wake depth, or turbulent intensity within the wake. Figure 12 indicates that a greater distance reduces the level of the heat transfer seemingly in an insignificant manner, in spite of the fact that a wake width in terms of velocity is almost proportional to  $\sqrt{l_b}$  and the change in the distance  $l_b$  from 0.06 m to 0.24 m results in a doubled wake width. In this sense, the greater distance and the wider wake do not appear to play a significant role in the unsteady heat transfer of the present case.

#### 4.3 Evaluation of the forced transition models

From Eq. (12), the intermittency factor  $\gamma(x)$  is calculated from the measured heat transfer data as

$$\gamma(x) = \frac{St(x) - St_L(x)}{St_T(x) - St_L(x)}. \quad (13)$$

Fitting a curve of the Eq. (1) as well as Eq. (4) on the obtained heat transfer data, we have determined a starting point of the forced transition  $x_{TW}$  and/or the coefficient  $C$  in Eq. (4). According to the study by Hodson<sup>(13)</sup>, the propagation speeds of the leading and the trailing edges of the turbulent spot are assumed to be  $1.0U_\infty$  and  $0.55U_\infty$ , respectively. It should be noted that no trials for the above-mentioned curve fitting yielded reasonable results for the Mayle-Dullenkopf model (Eq. (4)) in the higher wake frequency condition.

It is consequently found that the starting point locates around  $x/L=0.04$ , at which the momentum thickness Reynolds number,  $Re_{\theta}$  is estimated to be about 190 provided that the initial velocity profile is the Blasius solution. It should be mentioned that this value is very close to 200, which corresponds to the instability point of the laminar boundary layer with no pressure gradient. Figure 13 shows that the coefficient  $C$  of Eq. (4) is no longer constant but strongly depends on the wake frequency, while Mayle and

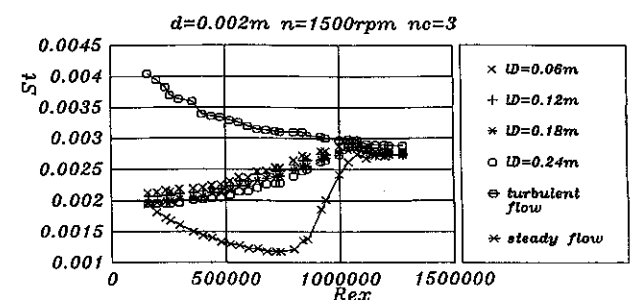


Fig. 12 Effect of the cylinder and the plate on the time-averaged Stanton number distribution

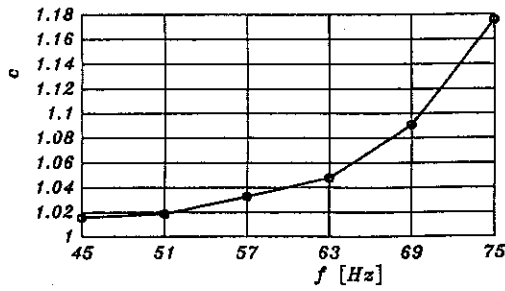


Fig. 13 Dependency of the coefficient  $C$  on the wake frequency

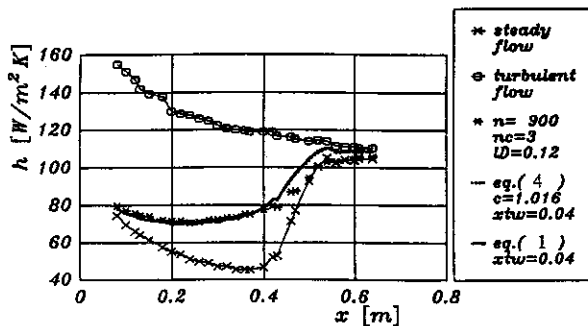


Fig. 14 Predictions of the heat transfer distribution by the two different wake-induced transition models ( $n=900$  rpm,  $n_c=3$ )

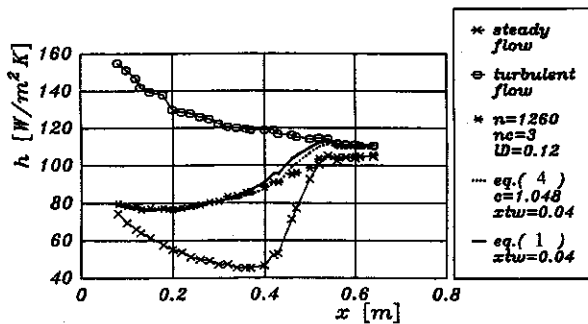


Fig. 15 Predictions of the heat transfer distribution by the two different wake-induced transition models ( $n=1260$  rpm,  $n_c=3$ )

Dullenkopf recommend a fixed value ( $=1.9$ ) for this coefficient. Figures 14 - 17 show some of the comparisons between the experimental data and the estimation curve of Eq. (12) using Eq. (1) (solid line), and the curve of Eq. (4) with the corresponding coefficient  $C$  (broken line). All curves represent the experimental data fairly well but slight differences appear near the end of the forced transition in all figures, which is probably due to the existence of the steady transition and is not very significant in practical situation. As mentioned above, in spite of many trials for the curve fitting, Eq. (11) with the model of Eq. (4) in higher wake frequencies failed to provide any satisfying results, as seen in Fig. 17.

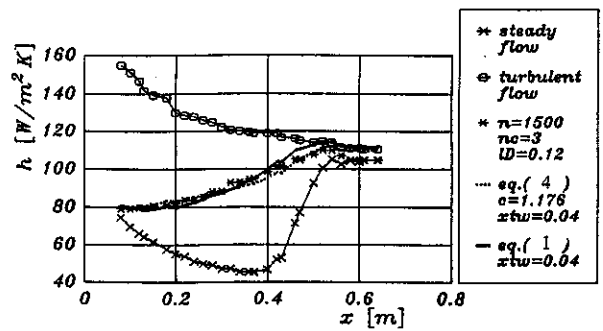


Fig. 16 Predictions of the heat transfer distribution by the two different wake-induced transition models ( $n=1500$  rpm,  $n_c=3$ )

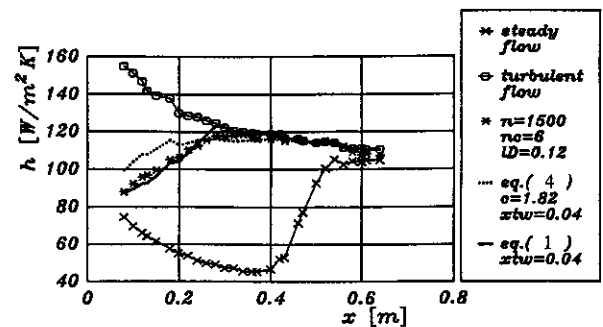


Fig. 17 Predictions of the heat transfer distribution by the two different wake-induced transition models ( $n=1500$  rpm,  $n_c=6$ )

### 5. Discussion

Two forced transition models of a wake-induced unsteady boundary layer, Eq. (1) and Eq. (4), were examined with respect to reproduction of the obtained heat transfer data by those models. It is found that both models yield almost the same results except for the highest-frequency case adopted in this study. One should recall again that the Mayle-Dullenkopf model employs a constant coefficient  $C$ , in contrast with the experimental observation that the coefficient varies with the unsteady flow condition, mainly, the wake frequency. Moreover, they did not specify any methods for obtaining the starting point of the forced transition, which is a very critical factor in predicting the wake effect on the heat transfer. The present authors feel, from the observations in this study, that the forced transition is related to the instability point of the laminar boundary layer, at which the momentum thickness Reynolds number becomes about 200.

It should be mentioned that the experiment was conducted under low turbulence intensity conditions, so that the effect of the natural transition was minimum, which made it possible to predict the time-averaged transitional behavior of the boundary layer with a very simple model. This is not always the case for the flow field in actual aero-engines because such

a flow field is very complicated and involves very high turbulence motions. Therefore it remains necessary to investigate more realistic simulated flow cases for wake/blade interaction problems.

### 6. Conclusions

Experimental simulation of the wake/blade interaction phenomena was made to investigate the effects of incident wakes on the characteristics of the transitional boundary layer on a flat plate. Findings of the study are summarized as follows,

(1) Incoming periodic wakes promote earlier transition of the boundary layer to increase the heat load level, i.e., Stanton number, over the plate, and this effect becomes more prominent for higher wake frequencies.

(2) Within the range of the test conditions in this paper, wake characteristics had no significant influence on the increase in the Stanton number.

(3) Two models for the forced transition of the boundary layer, the Pfeil model and the Mayle-Dullenkopf model, both of which are expressed in terms of the intermittency factor, were examined by comparison with the experimental data obtained in this study. Consequently, it was found that these two models provide almost the same prediction of the Stanton number distribution over the flat plate subjected to the periodic wakes, but in the higher frequency cases the Mayle-Dullenkopf model is less accurate in the prediction, compared to the Pfeil model.

### Acknowledgments

The authors would like to thank Professor Terukazu Ota of Tohoku University and Associate Professor Masaki Ohuchi, Iwate University for their advice in construction of the experimental setup and some of the measuring techniques. Assistance from Mr. Junichi Sakata and Mr. Yoshihiro Yamashita is also gratefully acknowledged.

### References

(1) Pfeil, H., Herbst, R. and Schroder, T., Investiga-

tion of the Laminar-Turbulent Transition of Boundary Layers Disturbed by Wakes, *Trans. ASME, J. Eng. Power*, Vol. 105 (1983), p. 130.

- (2) Addison, J.S. and Hodson, H.P., Unsteady Transition in an Axial-Flow Turbine: Part I—Measurements on the Turbine Rotor, *Trans. ASME, J. Turbomachinery*, Vol. 112 (1990), p. 206.
- (3) Addison, J.S. and Hodson, H.P., Unsteady Transition in an Axial-Flow Turbine: Part II—Cascade Measurements and Modeling, *Trans. ASME, J. Turbomachinery*, Vol. 112 (1990), p. 216.
- (4) Obremski, H.J. and Fejer, A.A., Transition in Oscillating Boundary Layer Flows, *J. Fluid Mech.*, Vol. 18 (1964), p. 438.
- (5) LaGraff, J.E., Ashworth, D.A. and Schultz, D.L., Measurement and Modeling of the Gas Turbine Blade Transition Process as Disturbed by Wakes, *Trans. ASME, J. Turbomachinery*, Vol. 111 (1989), p. 315.
- (6) Emmons, H.W., The Laminar-Turbulent Transition in a Boundary Layer—Part I, *Journal of Aeronautical Science*, Vol. 18 (1951), p. 490.
- (7) Narasimha, R., The Laminar-Turbulent Transition Zone in the Boundary Layers, *Proceedings Aerospace Science*, Vol. 22 (1985), p. 22.
- (8) Mayle, R.E. and Dullenkopf, K., A Theory for Wake-Induced Transition, *ASME Paper 90-GT-57*, (1989).
- (9) Mayle, R.E. and Dullenkopf, K., More on the Turbulent-Strip Theory for Wake-Induced Transition, *ASME Paper 90-GT-137*, (1990).
- (10) Young, A.D., Boundary Layer, *AIAA Education Series*, (1989), AIAA, p. 131.
- (11) Kline, S.J. and McClintock, F.A., Describing Uncertainties in Single Sample Experiments, *Mechanical Engineering*, (1953), p. 3.
- (12) Meyer, R.X., The Effect of Wakes on the Transient Pressure and Velocity Distributions in Turbomachines, *Trans. ASME, Journal of Basic Engineering*, Vol. 80 (1957), p. 1544.
- (13) Hodson, H.P., Modeling Unsteady Transition and Its Effect on Profile Loss, *Trans. ASME, J. Turbomachinery*, Vol. 112 (1990), p. 619.